

# Texture Mapping by Isometric Spherical Embedding for the Visualization and Assessment of Regional Myocardial Function

Yechiel Lamash<sup>1</sup>, Anath Fischer<sup>1</sup>, and Jonathan Lessick<sup>2</sup>

<sup>1</sup> Technion—Israel Institute of Technology, Haifa 32000, Israel

<sup>2</sup> Rambam - Health Care Campus, Haifa, Israel

**Abstract.** In the current study we show how texture mapping to the surface of the heart's left ventricle(LV) can be used to demonstrate the ventricle's complex kinematics and highlight impaired regions. The method uses isometric spherical embedding to map a uniform and oriented texture into a reference phase of the LV's mesh. The texture, attached to the deformed mesh, deforms with it and allows the visualization of rotation, strain and torsion in the circumferential and longitudinal coordinates. Such visualization demonstrates the absolute and relative values of these kinematic parameters and aids in the assessment of regional myocardial function.

## 1 Introduction

Cardiac pathologies such as myocardial ischemia are generally associated with regional ventricular dysfunction. The contraction of the heart's left ventricle (LV) is strongly related to its unique structure of fibers, allowing it to deform simultaneously in the longitudinal, radial, and circumferential directions. Noninvasive assessment of global and regional myocardial function provides valuable information for detecting and staging cardiac pathologies. Major effort is currently invested in developing methods for accurate 3D tracking of the left ventricle from images acquired by various imaging modalities (Echo, MR, CT). The results of these methods require 4D visualization techniques that can demonstrate the complex kinematics of the myocardium. In current usage, the resulting kinematic parameters (e.g. displacement, velocity and strain) are demonstrated separately by color maps or graphs. Each parameter is scaled according to absolute standard values or as a relative distribution. Thus, the relative part of each parameter is not always clear. Different parameters are sometimes contradictory, making it hard to determine the true regional function. In the current study we propose a texture mapping method for demonstrating the complex kinematics of the left ventricle at once, in a single view.

Texture mapping, in which an image is mapped onto a surface and deforms with it, is a fundamental technique in computer graphics and animation. The

problem of texture mapping is closely related to the embedding of high dimensional data in a low dimensional space, such that a certain distortion measure is minimized. Uniform textures such as checkerboards are generally used for visualizing embedding errors (distortions). However, when the embedding error is very small compared to the object's deformation, such a texture can be utilized to reliably demonstrate the deformation. Since the heart's LV is close in shape to a sphere, spherical embedding may be advantageous since it can be obtained without partitioning the surface and with less distortion. Several main approaches [11] have been introduced for the problem of isometric spherical embedding. One approach aims at finding a bijective map while minimizing length distortions. Several methods of this approach split the mesh into two, map the cut onto a great circle and embed each half-mesh onto a hemisphere. Each half-mesh can be embedded using a planar embedding [6,10] followed by a stereographic projection. The disadvantage of these methods is the introduction of discontinuities near the partition cuts, which in the current context can be falsely interpreted as deformations. Another approach for isometric spherical embedding uses multi-resolution techniques. These methods [9] start by simplifying the model until it becomes a tetrahedron, trivially embed it on the sphere, and then progressively add back the vertices with local vertex relaxation aimed at minimizing the stretch metric. However, this approach is limited to genus-0 surfaces. Constraining genus-zero topology to the left ventricle may result in larger distortions. In another approach [5,2], geodesic distances between pairs of points on the surface are first computed. Then, Multi-Dimensional Scaling (MDS) is applied to minimize the distortion of geodesic distances in the embedding spherical space. The presented method belongs to this approach.

Several optimization methods were used for solving the spherical MDS problem. Elad et al., [5] used gradient descent with line search in a multi-resolution framework. Bronstein et al., [2] used the BFGS quasi-Newton optimization for embedding of facial surfaces into  $S^3$ . These optimizations generally require large computation time. Another approach for solving MDS with less computation time is by SMACOF (Scaling by Minimization of Convex Function) [4]. SMACOF is a widely used gradient-descent algorithm for solving the MDS into Euclidean space that guarantees a monotonic decreasing convergence to the local minimum. Since some distances are monotonic with Euclidean distance, an effort was made to generalize SMACOF to solving non-Euclidian MDS problems. One such approach is to add various constraints to the MDS functional. For spherical MDS, a constraint that all the points be equi-distant from a central point was suggested by [1].

The current study proposes a texture mapping technique for demonstrating the complex kinematics of the LV in a single view. The method performs isometric spherical embedding of the endocardial LV surface using a constrained MDS approach. A fast approximation to the embedding radius is suggested and several optional textures are investigated. The current article is organized as follows: Section 2 describes the formulation of spherical embedding using MDS, including SMACOF algorithm and its expansion to spherical embedding. Section 3

demonstrates the results of the algorithm on disk and genus-zero topologies. The deforming texture on the LV endocardial surface of different heart phases is also demonstrated.

## 2 Method

The subendocardium is vulnerable to change early in the course of disease for a number of reasons. It is the layer furthest from the coronary blood supply. Moreover, it undergoes extreme transitions in pressure and compression in both the contraction (systole) and relaxation (diastole) phases, and it also appears prone to early structural microvascular architectural change such as fibrosis. Thus, the subendocardium is often the earliest myocardial layer affected in many disease processes [12]. This observation suggests that the regional measurement of contraction in the endocardial surface can serve as an indication for early diagnosis of cardiac diseases. Therefore, the following analysis refers to the LV's endocardial surface.

### 2.1 Isometric Spherical Embedding of LV's Subendocardial Surface

We begin the analysis with a 4D point cloud or mesh of the LV's endocardial surface. The points or vertices represent physical locations on the LV and may be obtained by various tracking techniques applied to any Echo MR and CT image data. The data is initially transformed into the heart axis system in order for the texture to be appropriately mapped. The second-order geometric moments [3] can be used to find the principal directions. In case of a point cloud, a surface mesh is reconstructed to the 3D points of reference phase. A relaxed phase should be selected rather than a contracted phase, since the shape is closer to a sphere and the points are more equidistant, a feature that is useful both for better embedding and for better triangulation. The mesh can have either disk or zero-genus topology, with preference to geodesic-convex disk topology since this may yield less embedding error. In the next stage, spherical embedding of the reference mesh is performed. Isometric embedding is used to preserve distances, so that the relative deformation will be consistent with the regional true strain. A texture with a uniform oriented pattern is then mapped onto the reference mesh. We assume that the embedding error is very small compared to the LV deformation. This allows the attached texture to deform with the mesh and demonstrates the regional rotation, strain and torsion. The next section describes the process of isometric spherical embedding using MDS which requires the computation of geodesic distances between the vertices. An efficient algorithm for computing geodesic distances on triangulated manifolds is the Fast Marching Method [7].

### 2.2 Isometric Spherical Embedding Using MDS

We start this section by describing the mathematical formalism of MDS.

Given a shape  $X$  and a metric  $d_X$  with the shortest distances between the surface points, find a map  $f : (X, d_X) \rightarrow (S^m, d_s)$  such that  $d_X(x, x') = d_s(f(x), f(x'))$  for all  $x, x' \in X$ .

It can be shown [8] that even a very simple discrete metric space consisting of only four points cannot be isometrically embedded into a space of constant Gaussian curvature of any finite dimension. However, by allowing small distortions we can still obtain a representation of the surface in an embedded space.

The MDS  $L_2$  norm minimization can be expressed as:

$$\sigma_2(Z) = \operatorname{argmin}_{f: X \rightarrow S^2} \sum_{i>j} |d_S(z_i, z_j) - d_X(x_i, x_j)|^2 \tag{1}$$

A two-dimensional sphere can be parameterized by a pair of coordinates  $(u^1, u^2) \in [0, 2\pi) \times [-\frac{\pi}{2}, \frac{\pi}{2}]$ .

The corresponding vector in  $R^3$  is given by:

$$\begin{aligned} z^1(u^1, u^2) &= r \cos(u^1) \cos(u^2) \\ z^2(u^1, u^2) &= r \sin(u^1) \cos(u^2) \\ z^3(u^1, u^2) &= r \sin(u^2) \end{aligned} \tag{2}$$

The shortest path between two points on the sphere’s surface is a segment of a planar section of the sphere, called the great circle. The geodesics on the sphere are therefore arcs centered at the origin. The geodesic distance between any two points  $u$  and  $u'$  on the sphere is given by the length of the arc connecting them,

$$d_S(u, u') = r \cdot \arccos\left(\frac{z(u)^T z(u')}{r^2}\right) \tag{3}$$

### 2.3 SMACOF Algorithm

The current section describes the SMACOF algorithm for solving the MDS problem.

The MDS  $L_2$  stress expression can be written in a more convenient matrix form,

$$\sigma_2(Z) = \operatorname{trace}(Z^T V Z) - 2\operatorname{trace}(Z B(Z; D_x) Z) + \sum_{i>j} d_X^2(x_i, x_j) \tag{4}$$

where,  $V$  is a constant  $N \times N$  matrix with elements

$$v_{ij} = \begin{cases} -1 & \text{if } i \neq j; \\ N - 1 & \text{if } i = j. \end{cases}$$

and  $B(Z; D_x)$  is an  $N \times N$  matrix depending on  $Z$  and  $D_x$  with elements,

$$b_{ij}(Z; D_x) = \begin{cases} -d_X(x_i, x_j) d_{ij}^{-1}(Z) & \text{if } i \neq j \text{ and } d_{ij}^{-1}(Z) \neq 0; \\ 0 & \text{if } i \neq j \text{ and } d_{ij}^{-1}(Z) = 0; \\ \sum_{k \neq i} b_{ik} & \text{if } i = j. \end{cases}$$

The gradient of  $f$  with respect to  $Z$  is,

$$\nabla_Z \sigma_2 = 2VZ - 2B(Z; D_x)Z \tag{5}$$

Jan De Leeuw [4] noticed that  $trace(ZB(Z; D_x)Z)$  is bounded below by  $trace(ZB(Q; D_x)Q)$  for all  $Q \in R^{m \times n}$ . This observation leads to the inequality:

$$\begin{aligned} h(Z, Q) &= trace(Z^T VZ) - 2trace(ZB(Q); D_x)Q + \sum_{i>j} d_X^2(x_i, x_j) \\ &\geq trace(Z^T VZ) - 2trace(ZB(Z^{(k)}; D_x)Z^{(k)}) + \sum_{i>j} d_X^2(x_i, x_j) \end{aligned} \tag{6}$$

The function  $h(Z, Q)$  is convex and quadratic with respect to  $Z$ , that touches  $\sigma_2(Z)$  at the point  $Q = Z$ . Therefore,  $h(Z, Q)$  serves as a majorizing function for  $\sigma_2(Z)$ .

By using the iterative majorization algorithm for minimizing the stress, at the  $(k + 1)^{st}$  iteration, the solution  $Z^{(k+1)}$  is found as the minimizer of  $h(Z, Z^{(k)})$ . Since the majorizing function is quadratic the minimizer can be obtained analytically by imposing  $2VZ - 2B(Z^{(k)}; D_x)Z^{(k)} = 0$ .

By rearranging the expression we obtain the update rule

$$Z^{(k+1)} = V^\dagger B(Z^{(k)}; D_x)Z^{(k)} \tag{7}$$

where,  $V^\dagger$  is the pseudo inverse of  $V$ .

### 2.4 Generalizing SMACOF to Spherical Embedding

In order to generalize SMACOF to spherical spaces [1], an extra point  $x_0$  is introduced into the MDS problem requiring all points to be equi-distant from it.

$$\sigma(Z) = \min \sigma_2(X, D_x) + k \cdot \min \sigma_C(X, D_{x_0}) \tag{8}$$

where,  $\sigma_C$  is the constraint on the distances from  $x_0$  and  $k$  is a non-negative penalty parameter. The update formula becomes

$$Z^{(k+1)} = (V + k \cdot I)^{-1}(VZ^{(k)} - \hat{Z}^{(k)}) \tag{9}$$

where,  $\hat{z}_l^{(k)} = r \frac{\hat{z}_l^{(k)}}{\|\hat{z}_l^{(k)}\|}$ .

### 2.5 Selection of Embedding Radius

Bronstein et al. [3] showed a procedure for calculating the optimal embedding in which the MDS was run over a grid of radiuses and then the radius with the minimal stress was selected. While this process assures an optimal selection of embedding radius, it might also take a long runtime. Since in our case the LV

surface is not far from a spherical shape, a good approximation to the optimal radius can be made.

Notice that  $\arccos(\frac{z(u)^T z(u')}{r^2}) = \arccos(\frac{z(u)^T z(u')}{\|Z^T\| \|Z\|})$ , we can therefore switch between the two expressions.

We assume that the vertices are close to their final position; thus, by freezing them a quadratic expression for the stress with respect to  $r$  is obtained:

$$\begin{aligned} \sum (d_S - d_X)^2 &= \sum_{i>j} (r \cdot \arccos(\frac{z(u)^T z(u')}{\|Z^T\| \|Z\|}) - d_X)^2 \\ &= \sum_{i>j} (\arccos(\frac{z(u)^T z(u')}{\|Z^T\| \|Z\|}) \cdot r^2 - 2 \arccos(\frac{z(u)^T z(u')}{\|Z^T\| \|Z\|}) d_X \cdot r + d_X^2) \\ &= r^2 \cdot \sum_{i>j} (\arccos(\frac{z(u)^T z(u')}{\|Z^T\| \|Z\|})) - 2r \cdot \sum_{i>j} \arccos(\frac{z(u)^T z(u')}{\|Z^T\| \|Z\|}) d_X + \sum_{i>j} d_X^2 \end{aligned} \quad (10)$$

A minimum is obtained at:

$$r_{min} = \frac{\sum_{i>j} \arccos(\frac{z(u)^T z(u')}{\|Z^T\| \|Z\|}) d_X}{\sum_{i>j} (\arccos(\frac{z(u)^T z(u')}{\|Z^T\| \|Z\|}))} \quad (11)$$

### 3 Experiments

We ran the algorithm on several surfaces of the LV reconstructed from computed tomography (CT) image data. Figure 1 demonstrates the spherical embedding of the genus-zero surface with color mapping of the rendered mean curvature of the trabeculle and papillary muscles. Figure 2 show the mapping of the checkerboard texture on the disk topology surface of the LV at phase 0% (left-most) and its propagation to the rest of the cardiac phases. Figure 3 demonstrates color coding of principal strains of the LV surface, with and without fusing it with a grid texture.

### 4 Discussion and Conclusions

The current study proposes a texture mapping technique for demonstrating the complex kinematics of the LV. The method performs isometric spherical embedding of the endocardial LV surface using a constrained MDS approach. The visualization of the complex kinematics, as seen in Figure 2 and Figure 3, becomes easier when running a movie of the deforming surface with checkerboard texture. We also tested vertical lines texture and soccer ball texture, but the deformation was less apparent with them. Mapping of the 17-segments bull's-eye image on a patient's LV surface as demonstrated in Figure 4, show how results from different modalities can be fused and analyzed with a pixelwise correspondence. We conclude that mapping a uniform texture into the reference phase of a deformed object is an efficient way to demonstrate its deformation and thus can aid in assessing regional myocardial function.

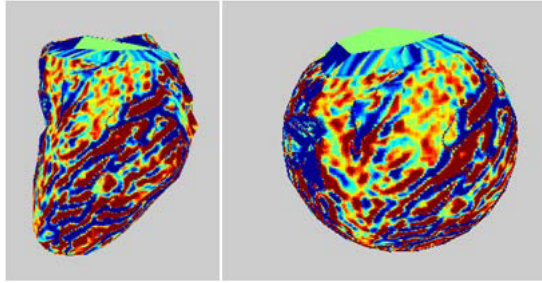


**Fig. 1.** Left ventricle endocardial genus-0 surface mesh of 200 vertices before (left) and after (right) spherical embedding. The colored texture is a projection of the mean curvature of the trabeculle and papillary muscles on mesh faces. The green area is the septum.



**Fig. 2.** Mapping of checkerboard texture on phase 0%. The texture deformation during the contraction and back to relaxation (from left to right) demonstrates the LV strain and torsion. The mid-apex part shows more circumferential strain compared to the mid-base.

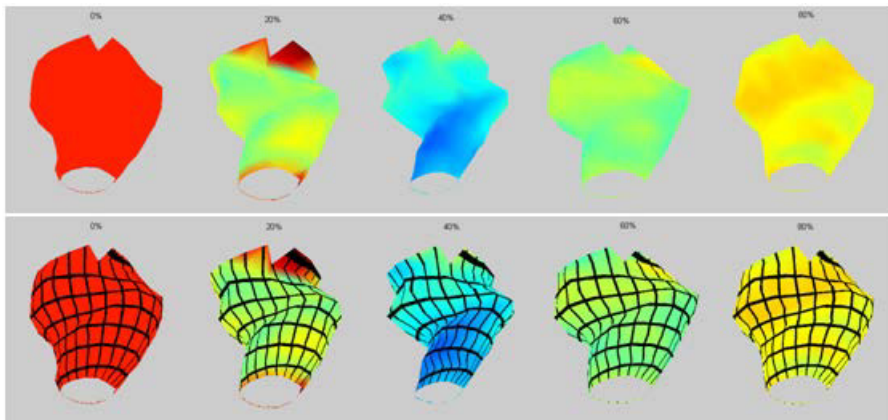


**Fig. 3.** Upper: principal strain in color (scale of blue to red strain values are  $[-0.5, 0.1]$ ). The principal strain was calculated from the mesh with respect to phase 0%. Lower: fusion of grid texture (mapped on phase 0%) with principal strain. The grid texture highlights the LV's strain and torsion.

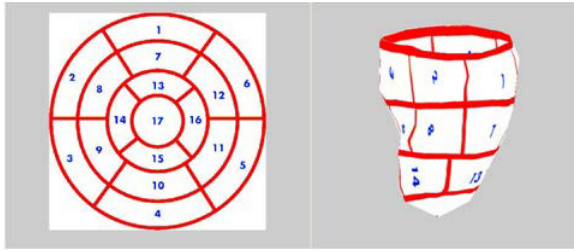


**Fig. 4.** An image of the 'AHA17-segments' was mapped into a patient's LV surface mesh

## References

1. Borg, I., Lingoes, J.C.: A model and algorithm for multidimensional scaling with external constraints on the distances. *Psychometrika* 45(1), 25–38 (1980)
2. Bronstein, A.M., Bronstein, M.M., Kimmel, R.: Isometric embedding of facial surfaces into formula\_image. In: Kimmel, R., Sochen, N.A., Weickert, J. (eds.) *Scale-Space 2005*. LNCS, vol. 3459, pp. 622–631. Springer, Heidelberg (2005)
3. Bronstein, A.M., Bronstein, M.M., Kimmel, R.: *Numerical geometry of non-rigid shapes*. Springer (2008)
4. De Leeuw, J.: *Multidimensional scaling* (2011)
5. Elad, A., Kimmel, R.: Spherical flattening of the cortex surface. In: *Geometric Methods in Bio-medical Image Processing*, pp. 77–89 (2002)
6. Gotsman, C., Gu, X., Sheffer, A.: Fundamentals of spherical parameterization for 3d meshes. *ACM Transactions on Graphics (TOG)* 22, 358–363 (2003)
7. Kimmel, R., Sethian, J.A.: Computing geodesic paths on manifolds. *Proceedings of the National Academy of Sciences* 95(15), 8431–8435 (1998)
8. Morrison, A., Ross, G., Chalmers, M.: Fast multidimensional scaling through sampling, springs and interpolation. *Information Visualization* 2(1), 68–77 (2003)
9. Praun, E., Hoppe, H.: Spherical parameterization and remeshing. *ACM Transactions on Graphics (TOG)* 22(3), 340–349 (2003)
10. Saba, S., Yavneh, I., Gotsman, C., Sheffer, A.: Practical spherical embedding of manifold triangle meshes. In: *2005 International Conference on Shape Modeling and Applications*, pp. 256–265. IEEE (2005)
11. Sheffer, A., Praun, E., Rose, K.: Mesh parameterization methods and their applications. *Foundations and Trends® in Computer Graphics and Vision* 2(2), 105–171 (2006)
12. Stanton, T., Marwick, T.H.: Assessment of subendocardial structure and function. *JACC: Cardiovascular Imaging* 33(8), 867–875 (2010)